Intermediate structure in the photoexcitation of $^{77}Se^m$, $^{79}Br^m$, and $^{137}Ba^m$

J. J. Carroll,[1] C. B. Collins,[1] K. Heyde,[2] M. Huber,[3] P. von Neumann-Cosel,[3] V. Yu. Ponomarev,[4] D. G. Richmond,[1] A. Richter,[3] C. Schlegel,[3] T. W. Sinor,[1] and K. N. Taylor[1]

[1]*Center for Quantum Electronics, The University of Texas at Dallas, P.O. Box 830688, Richardson, Texas 75083*

[2]*Institute for Theoretical Physics, Proeftuinstraat 86, B-9000 Gent, Belgium*

[3]*Institut für Kernphysik, Technische Hochschule Darmstadt, Schlossgartenstrasse 9, D-64289 Darmstadt, Germany*

[4]*Laboratory of Theoretical Physics, Joint Institute for Nuclear Research, Dubna, Head Post Office, P.O. Box 79, Moscow, Russia*

(Received 28 June 1993)

Continuing the systematic investigation into the photoexcitation of isomers over wide mass and energy ranges, the production of $^{77}Se^m$, $^{79}Br^m$, and $^{137}Ba^m$ was studied with the bremsstrahlung facility at the superconducting Darmstadt linear accelerator. These isomers have half-lives on the order of seconds. Excitation functions were measured for the (γ,γ') reactions populating the metastable states for energies of 2–7 MeV and the important intermediate states were identified. Nuclear structure calculations with the quasiparticle-phonon model for ^{79}Br and the particle- (hole-) core coupling approach for ^{137}Ba gave satisfactory descriptions for the strength and position of the dominant mediating levels. Admixtures of fragmented outershell single-particle strength shifted to low energies were identified as essential features of the wave functions of those states. Intermediate states in ^{77}Se displayed very large strengths compared to other isomers in the same mass region, providing further support for the correlation between integrated cross sections and ground state deformations recently discovered in the $A=160$–200 mass region. Such an enhancement would considerably improve the feasibility of a gamma-ray laser based on the sudden deexcitation of isomeric populations in deformed nuclei.

PACS number(s): 25.20.Lj, 27.50.+e, 27.60.+j, 21.90.+f

I. INTRODUCTION

It has been known for more than fifty years that nuclear isomers could be populated by (γ,γ') reactions, yet the greatest progress in the study of this process and the underlying nuclear structure has occurred in the past decade. To a large degree this renaissance has been driven by research directed towards determining the feasibility of a gamma-ray laser whose pump scheme [1,2] would rely on the resonant deexcitation of long-lived nuclear isomers through intermediate states (IS). Such research has required the systematic development of a database describing the population and depopulation of metastable levels. This effort began in earnest [3–10] in 1987 and has recently concentrated [11–16] on the investigation of IS in the largely unexplored excitation energy range of 2–6 MeV.

Applications notwithstanding, the photoactivation of isomers is important in its own right. For example, the integrated cross sections measured for IS can reveal interesting nuclear structures [17–19] since both strong absorption transitions from the ground state and significant cascades to the isomer are needed. In this regard the combination of photoactivation and nuclear resonance fluorescence (NRF) experiments has proven to be a particularly useful tool and the resulting information has been successfully compared with microscopic calculations [13,16]. For deformed nuclei a remarkable discovery [5,11,14] was the appearance of low-lying levels which efficiently couple ground states and isomers differing by as many as eight units in the quantum number K, the projection of the total angular momentum on the major nuclear axis. The properties of IS are important in nuclear astrophysics when stellar nucleosynthesis of a radioisotope is expected to branch to both ground state and isomer which have greatly differing lifetimes [9,11,20]. In a practical field, nuclides with well-known IS can be used to characterize intense bremsstrahlung produced by linear accelerators or pulsed-power machines [21–23].

The systematic investigation of the photoexcitation of isomers was continued in this work by the study of ^{77}Se, ^{79}Br, and ^{137}Ba whose isomers have half-lives on the order of seconds. In addition to the experimental data, nuclear structure calculations are presented for ^{79}Br and ^{137}Ba which permitted a detailed interpretation of the interplay between single-particle and collective properties that provided the observed intermediate states.

II. EXPERIMENTS

A. Methods

The experiments were performed using the injector of the superconducting continuous wave electron accelerator (S-DALINAC) at Darmstadt [24]. Bremsstrahlung for the experiments was produced by electrons which impinged on a 3 mm thick tantalum converter foil. The

TABLE I. Summary of the literature values [25] for the relevant nuclear parameters and transparencies for the escape of fluorescence photons from samples of the nuclides.

Nuclide	g.s. spin J^π	E_{iso} (keV)	Isomer spin J^π	$T_{1/2}$ (s)	Abundance (%)	Principal fluorescence (keV)	Transparency (%)
^{77}Se	$\frac{1}{2}^-$	162	$\frac{7}{2}^+$	17.4	7.6	161.92	76
^{79}Br	$\frac{3}{2}^-$	207	$\frac{9}{2}^+$	4.86	50.69	207.2	76
^{137}Ba	$\frac{3}{2}^+$	662	$\frac{11}{2}^-$	153.12	11.23	661.66	85

electron energies were measured before and after each exposure to an accuracy of 50 keV and were varied from $E_0=2$ to 7 MeV in step sizes of 125 and 250 keV. The proper beam alignment was insured by maximizing the dose registered in a remote ionization chamber which viewed only the central 12 mrad of the bremsstrahlung. Variations in all beam parameters were recorded during each exposure, including the total charge passed to the converter.

Targets consisted of elemental Se and compounds of LiBr and BaF_2 with typical masses of 3–6 g. The materials were contained in hollow aluminum cylinders with 3.5 cm length and 1.4 cm outer diameter. The samples were irradiated axially with their plane faces located 1.3 cm from the converter foil. Nominal electron beam currents were 5 μA and the exposure periods were typically twice the half-life of the isomer being investigated. At the end of each irradiation the samples were transported pneumatically to a well-type NaI(Tl) detector for counting as described in more detail in Refs. [15,16]. To improve the statistical accuracy of the data, measurements were repeated for up to sixteen cycles for each isotope and electron energy. A sample of elemental In was also irradiated at some energies for calibration.

The numbers of isomers produced by these exposures were determined from the counting rates measured in distinctive fluorescence lines. The γ-ray signatures and other relevant parameters for the isomers investigated here are summarized in Table I. The raw numbers of counts within peaks observed in pulse-height spectra were corrected in a standard fashion [15] to account for the isomer half-lives, the detection efficiencies, and the opacities of samples to the escape of fluorescence photons. A typical example of the data is shown in Fig. 1(a) and was obtained from a Se sample following its irradiation with bremsstrahlung having an end-point energy of $E_0=4$ MeV. The isomeric decay signature was clearly identified despite the relatively poor resolution of the NaI spectrometer. In addition to pulse-height spectra, a multichannel analyzer was used to obtain decay curves like that of Fig. 1(b). As shown, there was excellent agreement between measured and adopted [25] values for the isomeric half-lives.

B. Data analysis

Recent investigations have confirmed [11–16,26] that the population of isomers by (γ,γ') reactions at excitation energies below the photoneutron threshold proceeds by the process depicted schematically in Fig. 2. The figure identifies the relevant parameters including the natural width of the intermediate state Γ and the branching ratios b_0 and b_{iso} for decay from the IS directly to the ground state and by unknown cascade to the metastable level, respectively. Along with the Breit-Wigner cross section for the absorption transition, these form the integrated cross section for population of the isomer through the IS,

$$(\sigma\Gamma)_{iso}=\pi^2\left[\frac{\hbar c}{E}\right]^2\frac{2J_{IS}+1}{2J_0+1}b_0 b_{iso}\Gamma\ , \tag{1}$$

where J_{IS} and J_0 are the angular momenta of the IS and ground state, respectively, and E is the energy of the absorption transition. The integrated cross section is expressed in usual units of 10^{-29} cm^2 keV, equivalent to 0.01 eV b. This quantity is of primary importance for photoactivation studies since the normalized activation A_f giving the fractional yield of isomers produced by an

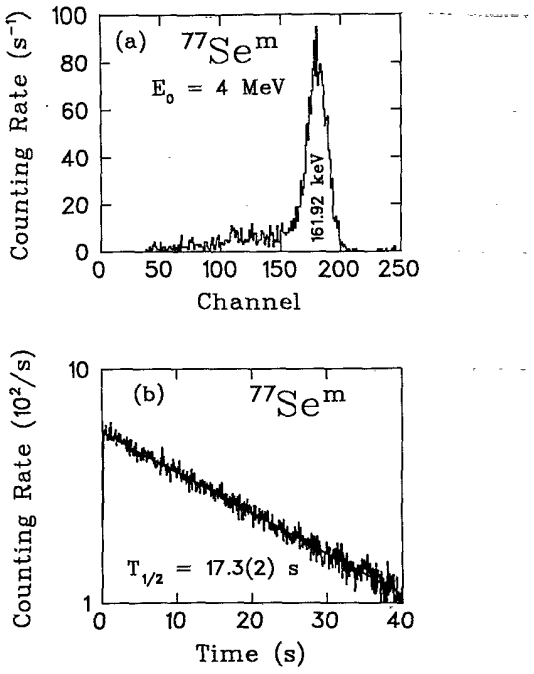

FIG. 1. (a) Pulse-height and (b) time-decay spectra obtained from a Se sample following its irradiation with bremsstrahlung having an end point of 4 MeV. The straight line in (b) represents a best fit (log scale) with $T_{1/2}=17.3\pm0.2$ s which agrees well with the literature value [25] of 17.45 s.

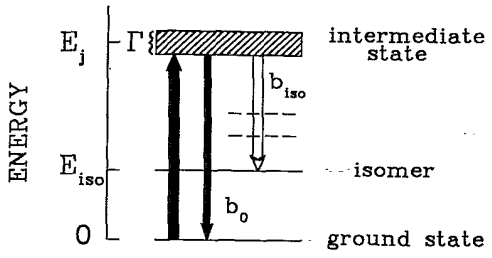

FIG. 2. Schematic representation of the resonant photoexcitation mechanism by which an isomer at an energy of E_{iso} is populated through the hatched intermediate state (IS). The IS is characterized by it excitation energy E_j and its natural width Γ. The branching ratios b_0 and b_{iso} describe the decay of the IS to the ground state and to the isomer, respectively. The latter quantity is the sum of all unknown cascades through the dashed levels which lead to the isomer.

irradiation per incident photon is

$$A_f=\frac{N_{iso}}{N_T\Phi_0}=\sum_j(\sigma\Gamma)^j_{iso}F(E_j,E_0)\ , \tag{2}$$

where N_{iso} is the number of isomers produced, N_T is the number of target nuclei, Φ_0 is the total photon flux for the specified end-point energy E_0, and $F(E_j,E_0)$ is the distribution of energies within the bremsstrahlung continuum normalized to 1. The summation in Eq. (2) allows the participation of a plurality of well-spaced gateways.

Values for Φ_0 and $F(E_j,E_0)$ were obtained for each end-point with the well-established EGS4 electron-photon transport code [27], as described in detail elsewhere [11–16]. The calculated spectra were validated with the $^{115}In(\gamma,\gamma')^{115}In^m$ reaction which is characterized sufficiently to serve as a calibration standard [13,23].

III. RESULTS

Figure 3 displays excitation functions of A_f vs end point for the production of $^{77}Se^m$, $^{79}Br^m$, and $^{137}Ba^m$. For comparison, the asterisks represent the experimental results obtained at $E_0=6$ MeV from Ref. [10]. The good agreement observed between values measured in completely different experimental environments established confidence in the procedures. Intermediate states were identified by sharp increases in the normalized activation. Integrated cross sections were then extracted by fitting Eq. (2) to the data in such a way as to minimize the residue,

$$R_M(E_0)=A_f(E_0)-\sum_{E_j=E_1}^{E_M}(\sigma\Gamma)^j_{iso}F(E_j,E_0)\ , \tag{3}$$

by successively removing contributions from the M lowest-lying IS.

End-point energies below 2 MeV were not accessible in the present work so previously measured experimental values for IS at lesser energies were included in the fitting procedure. In instances where literature values were unavailable or insufficient to reproduce the excitation functions of Fig. 3 up to the energy of the first visible IS, a single intermediate state was introduced at an excitation energy below 2 MeV. Its position and integrated cross section were chosen to remove the baseline level of activation and did not necessarily correspond to that of a real level. Properties of IS which reproduced the excitation functions measured here are summarized in Table II.

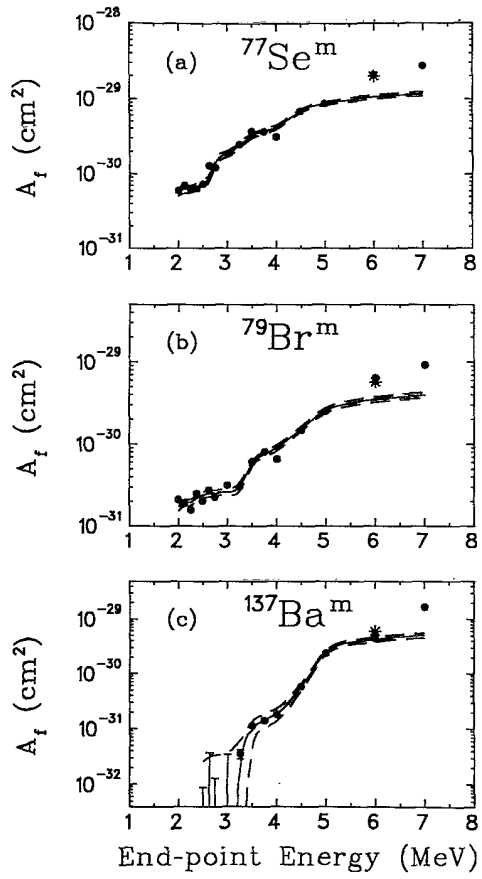

FIG. 3. Normalized yields A_f as functions of electron energy for the populations of (a) $^{77}Se^m$, (b) $^{79}Br^m$, and (c) $^{137}Ba^m$. The asterisks represent experimental results of Ref. [10] obtained at 6 MeV in a completely different environment and agree well with the present data. The solid lines correspond to excitation functions calculated using Eq. (2) with the intermediate states listed in Table II and the dashed lines describe the error bounds of this approach.

The ^{77}Se excitation function at low energies ($E_0\leq 2.6$ MeV) was partially reproduced by including the 30×10^{-29} cm^2 keV IS at 1.005 MeV of Anderson *et al.* [4], but neglecting the small contributions of the lower-lying levels listed there. The missing strength below 2 MeV was ascribed to an IS at 1.7 MeV of 150×10^{-29} cm^2 keV which served to remove the remaining baseline activation. Boivin *et al.* [28] also examined the production of this isomer up to an excitation energy of 1.7 MeV. Their work indicated three important IS at 1.000, 1.190, and 1.600 MeV with integrated cross sections of 3.2×10^{-29}, 18×10^{-29}, and 52×10^{-29} cm^2 keV, respectively. However, the yield calculated with these values severely underestimated the data. It is noteworthy that

TABLE II. Values of integrated cross sections $(\sigma\Gamma)^j_{iso}$ and excitation energies E_j of the intermediate states most important in the production of these isomers by (γ,γ') reactions. Values needed to fit the data were determined in this work by minimizing the residues of Eq. (5). Values available in the literature, where available, were used to reproduce the excitation functions for energies below that of IS clearly identified in this work. Strengths listed above 4 MeV were introduced to account for the excess yield observed toward higher energies and did not necessarily correspond to single levels or groups of levels. No error is given for the 2 MeV state in ^{137}Ba since this level was simply used to estimate the maximum strength corresponding to the baseline activation resulting from null measurements at $E_0 < 3$ MeV.

Isomer	E_j (MeV)	$(\sigma\Gamma)^j_{iso}$ (10^{-29} cm^2 keV)	
^{77}Se^m	1.005	30	Ref. [4]
	1.7±0.1	150±15	
	2.6±0.1	1200±120	
	3.2±0.1	3700±370	
	4.0±0.1	5500±1000	
^{79}Br^m	0.761	5.9	Refs. [3,4,29]
	1.8±0.1	65±6	
	3.2±0.1	850±90	
	4.4±0.2	7000±1500	
^{137}Ba^m	2.0	<15	
	3.2±0.1	220±20	
	4.5±0.2	8500±800	

when their integrated cross section at 1.005 MeV was replaced by that of Ref. [4], and with their values for IS at 1.190 and 1.600 MeV, good agreement was obtained between the calculated and measured excitation function below 2.6 MeV.

In the case of ^{79}Br, the well-known level [3,4,29] at 0.761 MeV was included as listed in Table II. The literature does not support the identification of any other IS up to an energy of 1.7 MeV. However, after removing the contribution from the above state the shape of the excitation function of Fig. 3(b) did not indicate a flat baseline but instead followed the isochromat [30] of an IS positioned near 2 MeV. Therefore a level was concluded to lie at 1.8±0.1 MeV as shown in the table.

The data displayed below 3 MeV in the excitation function for ^{137}Ba represent upper bounds on the yield obtained from null measurements for fluorescence from the isomer. This small baseline was consistent with an IS at 2 MeV with less than 15×10^{-29} cm^2 keV for its integrated cross section. For comparison a level at 1 MeV with less than 3×10^{-29} cm^2 keV would have also been allowed. The literature [31] describing excited states lying below 2.6 MeV does not support the identification of any IS so it was concluded that the first intermediate state of significant strength was located at 3.2±0.1 MeV.

The results of the application of Eqs. (2) and (3) that included the low-lying levels discussed above are shown as the solid lines in Fig. 3. The dashed lines define bands describing the errors in the values given in Table II and those quoted in the literature.

IV. MODEL CALCULATIONS

A. ^{79}Br

The photoexcitation of ^{79}Br^m, an odd-even nucleus, was studied in the quasiparticle-phonon model (QPM). The method for treating such nuclei in this theoretical framework is described in detail in Ref. [32] and has been successfully applied to the calculation of NRF and isomer photoexcitation [16] in ^{89}Y. Calculations of the properties of the ^{81}Br$(\gamma,\gamma')^{81}$Br^m reaction are also available [19] which should show very similar structure to those for ^{79}Br since both nuclei have the same g.s. and isomer spins. The two extra neutrons in ^{81}Br are not expected to significantly change the average field.

Calculations were performed with the wave function

$$\Psi_\nu(JM)=C^\nu_J\left[\alpha^\dagger_{JM}+\sum_{\lambda\mu i}D^{\lambda i}_j(J\nu)(\alpha^\dagger_{jm}Q^\dagger_{\lambda\mu i})_{JM}\right]\Psi_0\ , \qquad (4)$$

for states with angular momentum J and projection M. In Eq. (4), $\alpha^\dagger_{JM}$ denotes the one quasiparticle and $Q^\dagger_{\lambda\mu i}$ the phonon creation operator for angular momentum λ, projection μ, and random phase approximation root number i. The g.s. wave function of the even-even core is denoted by Ψ_0 and ν is the number within a sequence of states of given J^π.

The effective QPM Hamiltonian includes the average field, pairing interactions, and a residual interaction between quasiparticles. The latter was adjusted to reproduce the energy and strength of the 2^+_1 and 3^+_1 phonons in the neighboring even-even nuclei. A Woods-Saxon potential with the parametrization of Ref. [33] was used to describe the average field. Phonons with $J^\pi=1^\pm,2^\pm,3^\pm,4^\pm,5^-,6^+$, including the collective as well as two-quasiparticle states, were considered in the summation of the second term of Eq. (4). The complete configuration space up to $E_x=12$ MeV was taken into account to avoid truncation effects.

Numerical calculations were performed with the code PHOQUS [34]. The calculations were restricted to one-phonon coupled states, since the total electromagnetic

strength is known to be unaffected by the inclusion of multiphonon coupled configurations. An effective spin g factor $g^s_{\text{eff}}=(0.8)g^s_{\text{free}}$ was used. Effective charges $e^p_{\text{eff}}=(N/A)e$ and $e^n_{\text{eff}}=-(Z/A)e$ were introduced for $E1$ transitions to separate the central mass motion.

B. ^{137}Ba

The single-hole configuration of the unpaired neutron in ^{137}Ba relative to the $N=82$ shell closure suggested that the hole-core coupling model [35], called the unified model (UM), would be a useful approach. In the comparable case of ^{115}In (one proton hole relative to $Z=50$), encouraging results were obtained both for the description of NRF and for the isomer photoexcitation [13]. Also a detailed UM study of ^{143}Nd (one particle relative to $N=82$) has recently been reported which successfully accounted for all major features of the low-energy spectrum [36].

The configuration space consisted of 1h (one-hole) states (with respect to the semimagic ^{138}Ba nucleus) and 1p-2h (one-particle–two-hole) states (with respect to ^{136}Ba). The g.s. wave function of ^{136}Ba relative to the neutron closed shell at $N=82$ was calculated with the pairing interaction of the Hamiltonian. A realistic approximation to the ^{136}Ba g.s. wave function was essential, because important contributions to the electromagnetic excitations would have been missed using a simple pure two-hole $(s_{1/2})^{-2}_{0^+}$ configuration as suggested by the independent-particle model.

Single-particle energies were taken from systematics of the odd-mass Ba nuclei and the single-particle space was coupled to collective 2^+ and 3^- phonons in the neighboring even nuclei [37]. Excitation energies and transition strengths for those phonons were adopted from experimental data. The energy shift between 1h states and 1p-2h states across the shell closure was estimated from the neutron separation energy differences [35] between the ^{137}Ba and ^{139}Ba nuclei.

An effective charge $e^p_{\text{eff}}=(1.5)e$ and effective g factor $g^s_{\text{eff}}=(0.7)g^s_{\text{free}}$ were used for the calculations of electromagnetic transitions. A collective limit $g_R=Z/A$ was assumed for the gyromagnetic ratio. As was the case [13] for ^{115}In, strong transitions were hardly affected by using other g_R values, e.g., $g_R=0$.

The results of the UM calculations were validated against the low-energy spectrum [31] up to $E_x=2$ MeV. The $J^\pi=\frac{11}{2}^-$ isomer energy was found to be 150 keV too high, but this was sensitive to the $h_{11/2}$ single-particle energy and the 3^-_1 coupling strength in ^{136}Ba. Transitions between low-lying states ($E2$ transitions only) were reproduced within a factor of 2 for the scarce information available in the literature.

V. DISCUSSION

A. ^{77}Se

The nucleus ^{77}Se shows a very complex structure at low excitation energies [38,39] and no calculations are available for electromagnetic transitions above 1 MeV. The activation function in Fig. 3(a) is dominated by a transition at 2.6 MeV. The integrated cross section of Table II may be converted into a decay width and the corresponding reduced transition probabilities are $B(E1)\geq 2.9\times10^{-3}$ W.u., $B(M1)\geq 0.17$ W.u., and $B(E2)\geq 33.0$ W.u., depending on the assumed nature of the excitation step. These values are lower limits only, since the largest possible product of branching ratios, $b_0 b_{\text{iso}}=0.25$ was used. Typically, the branching ratio factor could be expected to be about 2–5 times smaller than this value.

It is interesting to note that yields obtained for ^{77}Se^m are much larger than those in other isomers in the same mass region (^{79}Br, ^{81}Br, ^{87}Sr, ^{89}Y). A large g.s. deformation ($\beta=-0.28$) has been derived [39] for ^{77}Se from Coriolis coupling calculations and therefore this provides another hint for the peculiar role of deformation in the variations of integrated cross sections for the population of isomers in different nuclei [15].

B. ^{79}Br

The ground state and isomer have spin structures of $\frac{3}{2}^-$ and $\frac{9}{2}^+$, respectively, so the isomer can be reached by either an $E2$ excitation to a $J^\pi=\frac{7}{2}^-$ IS followed by an $E1$ decay, or the reversed scheme of an $E1$ excitation to a $J^\pi=\frac{5}{2}^+$ IS with subsequent $E2$ decay. Intermediate states found in the QPM calculations are compared to the experimental data in Fig. 4 and show this behavior. Only two strong IS are observed and the contributions of all other levels are at least two orders of magnitude smaller.

A difficulty in the model results was the poor reproduc-

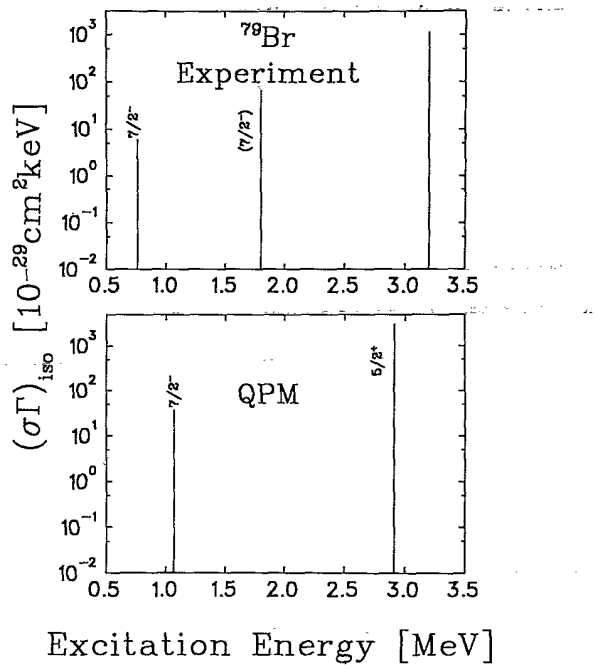

FIG. 4. Positions and strengths of intermediate states in ^{79}Br measured experimentally (upper) and calculated using the quasiparticle-phonon model as described in the text (lower).

tion of the $\frac{9}{2}^+$ isomer excitation energy, 1.270 MeV, which strongly distorted the energy-dependent integrated cross sections. Therefore, the experimental value of 0.127 MeV was used as the basis for electromagnetic transitions. A similar problem occurred in the ^{81}Br calculations [19]. There it was shown that the inclusion of two-phonon coupled configurations shifted the lowest $\frac{9}{2}^+$ state to roughly the correct position without strongly affecting the strength of the intermediate states.

The calculated low-energy IS has $J^\pi=\frac{7}{2}^-$, in agreement with the established 0.761 MeV level. Assuming the experimental 1.8 MeV state also to be $J^\pi=\frac{7}{2}^-$, a very good correspondence was obtained for the total energy-independent isomer population strength below $E_x=2$ MeV. Such a fragmentation would have naturally emerged from the model calculations if more complex configurations had been considered. Thus it was concluded that all IS below 2 MeV had $J^\pi=\frac{7}{2}^-$ and that the intermediate strength had a common excitation-decay structure.

The microscopic structure was extracted from the $\frac{7}{2}^-$ state wave function

$$\Psi_1(\tfrac{7}{2}^-)=(0.34)2f_{7/2}+(0.85)(2p_{3/2}\otimes 2_1^+)+\cdots .$$

The excitation occurred through the 2^+ phonon component coupled to the main g.s. configuration while the decay to the isomer took place in a $2f_{7/2}\rightarrow 1g_{9/2}$ $E1$ single-particle transition.

The strong experimental IS at 3.2 MeV was well reproduced by the QPM. The calculated $\sigma\Gamma$ was a factor of 3 larger, but again inclusion of many-phonon states would have been expected to bring the values into closer agreement. The QPM predicted $J^\pi=\frac{5}{2}^+$ for the IS and a reversed excitation-deexcitation sequence compared to the $\frac{7}{2}^-$ state. Analysis of the wave function

$$\Psi_1(\tfrac{5}{2}^+)=(0.38)2d_{5/2}+(0.90)(1g_{9/2}\otimes 2_1^+)\cdots$$

revealed that a $2p_{3/2}\rightarrow 2d_{5/2}$ $E1$ transition was responsible for the excitation and phonon coupling to the dominant isomer configuration provided an $E2$ decay.

The common feature in the intermediate levels of the QPM results is the presence of single-particle components in the wave functions belonging to strength having a centroid energy lying much higher. These configurations from the next major shell are strongly damped by coupling to collective excitations [32] and this pushes fragments to low energies. Exactly these components were found to be crucial for the isomer population in ^{79}Br.

C. ^{137}Ba

The experimental data showed evidence for only a single IS up to 4.3 MeV. Within the experimental limits, no contribution was observed below 2 MeV in agreement with the literature [31]. Thus, photoexcitation of ^{137}Ba^m has proven to be particularly important for the bremsstrahlung characterization technique of Ref. [22] since the isomer yield directly provides the photon flux at a single energy.

The results of the UM calculations are displayed in the middle part of Fig. 5 and indicate a strong transition at 2.75 MeV. Within the limitations of the model it appeared justified to assign this to the experimentally determined level 450 keV higher in energy at 3.2 MeV. The integrated cross section of the state was overpredicted by a factor of about 2–3, depending on whether the experimental or model excitation energy was used. However, similar to the ^{79}Br case this was probably due to the basis truncation and larger configuration spaces would be expected to bring the results closer to experiment.

An analysis of the wave functions of the IS identified $2d_{3/2}\rightarrow 2f_{5/2}$ single-particle $E1$ transitions as the common excitation mechanism. Because of the large spin difference, $\Delta J=4$ between g.s. and isomer, the decay occurs by complicated cascades which cannot be easily summarized.

A particular problem of the UM calculations already discussed for the ^{115}In$(\gamma,\gamma')^{115}$In^m reaction was a systematic deviation for the average $E1$ and $E2$ transition strengths with respect to experimental systematics in this mass region [40]. Good correspondence of the distribution shapes was obtained by comparing the reduced transition probabilities of all possible transitions up to 4 MeV in the model with Ref. [40]. However, the maximum had to be normalized with factors of $f(E1)=0.2$ and $f(E2)=50$ while absolute $M1$ strengths were reproduced well.

A reanalysis of the isomer population implementing

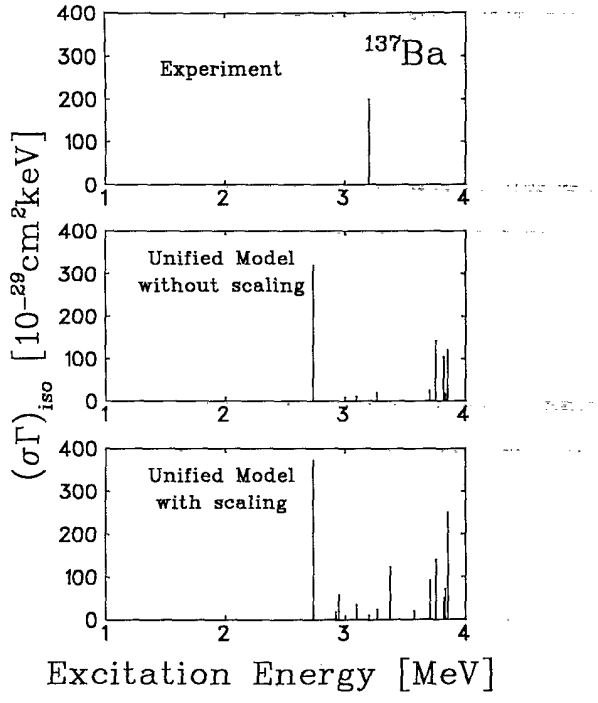

FIG. 5. Positions and strengths of intermediate states in ^{137}Ba measured experimentally (upper), calculated with the unified model (middle) and calculated with the unified model using empirically introduced correction factors for the average transition strengths (lower). Those factors were $f(E1)=0.02$ and $f(E2)=50$.

the normalization factors is shown in the lower part of Fig. 5. Surprisingly little change was observed with the main difference being some additional strength at 3–3.5 MeV. The $E2$ correction factor seemed unrealistically large considering how well the low-energy transitions were described. It is important to note that many of the weaker $E2$ transitions resulted from destructive interference of the collective and single-particle parts of the transition operator. The renormalization factor for $E1$ transitions seemed more realistic due to the sensitivity to smaller amplitudes of the wave functions which would have been smeared out in an enlarged configuration space. Accordingly, the best description might lie somewhere between the two extremes displayed in Fig. 5. However, the strong IS at 2.75 MeV which likely corresponds to the experimental 3.2 MeV level was hardly affected by these variations in the UM calculation.

VI. CONCLUSIONS

Excitation functions were measured for the photoactivation of $^{77}Se^m$, $^{79}Br^m$, and $^{137}Ba^m$ using bremsstrahlung with end-point energies in the range 2–7 MeV. This permitted the identification of intermediate states and the extraction of their integrated cross sections.

A particularly strong IS at 2.6 MeV was observed for the population of $^{77}Se^m$. Its transition strength significantly exceeds 10^{-3} W.u. for an $E1$ excitation or 0.1 W.u. for an $M1$ excitation, both of which are quite large values. In fact the magnitude of $^{77}Se^m$ yields compared to other isomers in this mass region provide further support for a correlation between integrated cross sections and the g.s. deformation. Such a correlation was recently discovered in the $A=160$–200 mass region [15] and is important to gamma-ray laser research since many candidate nuclei are well deformed.

The appearance of strong intermediate states requires a special combination of properties including a large partial g.s. width and significant mixing in the wave function. Thus the number of important levels is typically very small at energies below about 5 MeV as confirmed by the model results. The calculations further emphasized the importance of a delicate interplay of single-particle and collective amplitudes in the IS wave functions. In all examples analyzed so far (Refs. [13,19] and this work) the decisive factor has been the appearance of fragments of outer-shell single-particle strength at low energies. It would be of interest to compare these conclusions with findings in other valence-shell regions and in nuclei with large g.s. deformations. Experimental and theoretical work along these lines is underway.

ACKNOWLEDGMENTS

The authors gratefully acknowledge the valuable support of H.-D. Gräf and the S-DALINAC crew for providing excellent beams, W. Ziegler for assistance in conducting the experiments, and C. Spieler for help with the data analysis. One of us (P.v.N.-C.) would like to thank the group at the Center for Quantum Electronics for their hospitality during the stay when the present work was completed. This work was sponsored by the Department of Defense through the Naval Research Laboratory and the Bundesministerium für Forschung und Technologie, Contract No. 06DA641I. Partial support was received by NATO research Grant CRG92/0011 (K.H.) and by a grant of the Heisenberg-Landau program (V.Yu.P.).

[1] C. B. Collins, F. W. Lee, D. M. Shemwell, B. D. DePaola, S. Olariu, and I. I. Popescu, J. Appl. Phys. **53**, 4645 (1982).

[2] C. B. Collins, in *CRC Handbook of Laser Science and Technology, Supplement I: Lasers,* edited by M. J. Weber (CRC Press, Boca Raton, FL 1991), p. 561.

[3] J. A. Anderson and C. B. Collins, Rev. Sci. Instrum. **58**, 2157 (1987).

[4] J. A. Anderson and C. B. Collins, Rev. Sci. Instrum. **59**, 414 (1988).

[5] C. B. Collins, C. D. Eberhard, J. W. Glesener, and J. A. Anderson, Phys. Rev. C **37**, 2267 (1988).

[6] C. B. Collins, J. A. Anderson, Y. Paiss, C. D. Eberhard, R. J. Peterson, and W. L. Hodge, Phys. Rev. C **38**, 1852 (1988).

[7] J. A. Anderson, M. J. Byrd, and C. B. Collins, Phys. Rev. C **38**, 2838 (1988).

[8] J. A. Anderson, C. D. Eberhard, M. J. Byrd, J. J. Carroll, C. B. Collins, E. C. Scarbrough, and P. P. Antich, Nucl. Instrum. Methods **B40/41**, 452 (1989).

[9] J. J. Carroll, J. A. Anderson, J. W. Glesener, C. D. Eberhard, and C. B. Collins, Astrophys. J. **344**, 454 (1989).

[10] J. J. Carroll, M. J. Byrd, D. G. Richmond, T. W. Sinor, K. N. Taylor, W. L. Hodge, Y. Paiss, C. D. Eberhard, J. A. Anderson, C. B. Collins, E. C. Scarbrough, P. P. Antich, F. J. Agee, D. Davis, G. A. Huttlin, K. G. Kerris, M. S. Litz, and D. A. Whittaker, Phys. Rev. C **43**, 1238 (1991).

[11] C. B. Collins, J. J. Carroll, T. W. Sinor, M. J. Byrd, D. G. Richmond, K. N. Taylor, M. Huber, N. Huxel, P. von Neumann-Cosel, A. Richter, C. Spieler, and W. Ziegler, Phys. Rev. C **42**, 1813 (1990).

[12] J. J. Carroll, T. W. Sinor, D. G. Richmond, K. N. Taylor, C. B. Collins, M. Huber, N. Huxel, P. von Neumann-Cosel, A. Richter, C. Spieler, and W. Ziegler, Phys. Rev. C **43**, 897 (1991).

[13] P. von Neumann-Cosel, A. Richter, C. Spieler, W. Ziegler, J. J. Carroll, T. W. Sinor, D. G. Richmond, K. N. Taylor, C. B. Collins, and K. Heyde, Phys. Lett. B **266**, 9 (1991).

[14] J. J. Carroll, C. B. Collins, P. von Neumann-Cosel, D. G. Richmond, A. Richter, T. W. Sinor, and K. N. Taylor, Phys. Rev. C **45**, 470 (1992).

[15] C. B. Collins, J. J. Carroll, K. N. Taylor, D. G. Richmond, T. W. Sinor, M. Huber, P. von Neumann-Cosel, A. Richter, and W. Ziegler, Phys. Rev. C **46**, 952 (1992).

[16] M. Huber, P. von Neumann-Cosel, A. Richter, C. Schlegel, R. Schulz, J. J. Carroll, K. N. Taylor, D. G. Richmond, T. W. Sinor, C. B. Collins, and V. Yu. Ponomarev, Nucl. Phys. **A559**, 253 (1993).

[17] E. C. Booth and J. Brownson, Nucl. Phys. **A98**, 529 (1967).

[18] A. P. Dubenskij, V. V. Dubenskij, A. A. Boikova, and L.

Malov, Bull. Acad. Sci. USSR, Ser. Phys. **54**, 166 (1990).
[19] V. Ponomarev, A. P. Dubenskij, V. P. Dubenskij, and E. A. Boykova, J. Phys. G **16**, 1727 (1990).
[20] N. Klay, F. Käppeler, H. Beer, and G. Schatz, Phys. Rev. C **44**, 2839 (1991); K. T. Lesko, E. B. Norman, R.-M. Larimer, B. Sur, and C. D. Beausang, *ibid.* **44**, 2850 (1991).
[21] J. A. Anderson, C. D. Eberhard, K. N. Taylor, J. M. Carroll, J. J. Carroll, M. J. Byrd, and C. B. Collins, IEEE Trans. Nucl. Sci. **36**, 241 (1989).
[22] J. J. Carroll, D. G. Richmond, T. W. Sinor, K. N. Taylor, C. Hong, J. D. Standifird, C. B. Collins, N. Huxel, P. von Neumann-Cosel, and A. Richter, Rev. Sci. Instrum. **64**, 2298 (1993).
[23] P. von Neumann-Cosel, N. Huxel, A. Richter, C. Spieler, J. J. Carroll, and C. B. Collins (submitted to Nucl. Instrum. Methods).
[24] K. Alrutz-Ziemssen, D. Flasche, H-D. Gräf, V. Huck, M. Knirsch, W. Lotz, A. Richter, T. Rietdorf, P. Schardt, E. Spamer, A. Staschek, W. Voigt, H. Weise, and W. Ziegler, Part. Acc. **29**, 53 (1990).
[25] E. Browne and R. B. Firestone, in *Table of Radioactive Isotopes,* edited by V. S. Shirley (Wiley, New York, 1986); *Evaluated Nuclear Structure Data File* (Brookhaven National Laboratory, Upton, New York, 1986).
[26] P. von Neumann-Cosel, A. Richter, J. J. Carroll, and C. B. Collins, Phys. Rev. C **44**, 554 (1991).
[27] *Monte Carlo Transport of Photons and Electrons,* edited by T. M. Jenkins, W. R. Nelson, and A. Rindi (Plenum, New York, 1988).
[28] M. Boivin, Y. Cauchois, and Y. Heno, Nucl. Phys. **A137**, 520 (1969).
[29] B. Singh and D. A. Viggars, Nucl. Data Sheets **37**, 393 (1982).
[30] J. Guth, Phys. Rev. **59**, 325 (1941).
[31] L. K. Peker, Nucl. Data Sheets **59**, 767 (1990).
[32] S. Gales, Ch. Stoyanov, and A. I. Vdovin, Phys. Rep. **166**, 125 (1988).
[33] V. Yu. Ponomarev, V. G. Soloviev, Ch. Stoyanov, and A. I. Vdovin, Nucl. Phys. **A323**, 446 (1979).
[34] Ch. Stoyanov and C. Q. Khuong, JINR Dubna Report P-4-81-234, 1981 (unpublished).
[35] K. Heyde, P. van Isacker, M. Waroquier, J. L. Wood, and R. A. Mayer, Phys. Rep. **102**, 291 (1983).
[36] L. Trache, K. Heyde, and P. von Brentano, Nucl. Phys. **A554**, 118 (1993).
[37] S. Raman, W. C. Nestor, Jr., S. Kahane, and K. H. Bhatt, At. Data Nucl. Data Tables **42**, 1 (1989).
[38] S. L. Heller and J. N. Friedman, Phys. Rev. C **10**, 1509 (1974); **12**, 1006 (1975).
[39] S. E. Larsson, G. Leander, and I. Ragnarsson, Nucl. Phys. **A307**, 189 (1978).
[40] P. M. Endt, At. Data Nucl. Data Tables **26**, 47 (1981).